Biochimica et Biophysica Acta 1857 (2016) 1490–1496

Contents lists available at ScienceDirect

Biochimica et Biophysica Acta

journal homepage: www.elsevier.com/locate/bbabio

# Probing the pigment binding sites in LHCII with resonance Raman spectroscopy: The effect of mutations at S123

Elizabeth Kish [a,1], Ke Wang [b,1], Manuel J. Llansola-Portoles [a,*,1], Cristian Ilioaia [a], Andrew A. Pascal [a], Bruno Robert [a,2], Chunhong Yang [b,2]

[a] Institute for Integrative Biology of the Cell (I2BC), CEA, CNRS, Univ Paris-Sud, Université Paris-Saclay, F-91198 Gif-sur-Yvette cedex, France
[b] Key Laboratory of Photobiology, Institute of Botany, Chinese Academy of Sciences, Beijing 100093, PR China

ARTICLE INFO

*Article history:*
Received 7 April 2016
Received in revised form 31 May 2016
Accepted 2 June 2016
Available online 3 June 2016

*Keyword:*
Carotenoid
Electronic absorption
LHCII
Lutein
Neoxanthin
Resonance Raman

ABSTRACT

Resonance Raman spectroscopy was used to evaluate the structure of light-harvesting chlorophyll (Chl) *a*/*b* complexes of photosystem II (LHCII), reconstituted from wild-type (WT) and mutant apoproteins over-expressed in *Escherichia coli*. The point mutations involved residue S123, exchanged for either P (S123P) or G (S123G). In all reconstituted proteins, lutein 2 displayed a distorted conformation, as it does in purified LHCII trimers. Reconstituted WT and S123G also exhibited a conformation of bound neoxanthin (Nx) molecules identical to the native protein, while the S123P mutation was found to induce a change in Nx conformation. This structural change of neoxanthin is accompanied by a blue shift of the absorption of this carotenoid molecule. The interactions assumed by (and thus the structure of the binding sites of) the bound Chls *b* were found identical in all the reconstituted proteins, and only marginally perturbed as compared to purified LHCII. The interactions assumed by bound Chls *a* were also identical in purified LHCII and the reconstituted WT. However, the keto carbonyl group of one Chl *a*, originally free-from-interactions in WT LHCII, becomes involved in a strong H-bond with its environment in LHCII reconstituted from the S123P apoprotein. As the absorption in the $Q_y$ region of this protein is identical to that of the LHCII reconstituted from the WT apoprotein, we conclude that the interaction state of the keto carbonyl of Chl *a* does not play a significant role in tuning the binding site energy of these molecules.


## 1. Introduction

The first steps of photosynthesis involve the absorption of solar photons by specialized pigments located in the light-harvesting proteins of photosynthetic organisms. The excitation energy is efficiently transferred to reaction centers, where it is then converted into chemical potential energy. In green plants, light collection by photosystem II (*PSII*) is achieved by a highly complex antenna system involving many partner proteins — the major and minor light-harvesting chlorophyll (Chl) *a*/*b* complexes of *PSII* (LHCII and CP24, CP26 & CP29, respectively), and the inner antenna proteins (CP43 and CP47). LHCII is the most important complex involved in the process of light absorption, not only because it binds half of the Chls in the photosynthetic membrane, but also because it is involved in a number of regulatory mechanisms that ensure the plants' fitness under ever-changing environmental conditions. It is responsible for the partition of excitation energy between photosystems I and II according to light quality [1] through the so-called state transition, and is also responsible for the dissipation of excess excitation energy under high light conditions *via* the fast phase of non-photochemical quenching (NPQ) [2–4]. This membrane protein is naturally present as a trimer of subunits, encoded by a family of highly homologous nuclear genes (*lhcb1-3*) [5]. The spinach and pea LHCII structures have been resolved to 2.7 [6] and 2.5 [7] angström resolution, respectively. Each LHCII subunit possesses three transmembrane helices, and binds 14 Chls (8 Chls *a* and 6 Chls *b*) as well as four carotenoid molecules, two luteins, one neoxanthin (Nx), and one xanthophyll cycle carotenoid [6]. This structure provided an essential framework for modelling both the electronic properties of LHCII and the cascade of events following photon absorption in this protein (see *e.g.* [8]). However, the molecular events occurring in LHCII upon state transition or NPQ induction remain to be elucidated. The former requires LHCII phosphorylation, while the latter is proposed to occur *via* a conformational change in LHCII, from a state where it efficiently harvests solar photons to one in which it dissipates the excitation energy [1,3,4].

Generally, the engineering of a series of site-selected mutants designed to impair or modify the function of a given protein is of great help in understanding the molecular mechanisms underlying its

*Abbreviations:* Chl, chlorophyll; *PSII*, photosystem II; LHCII, light harvesting antenna complex of *PSII*; NPQ, nonphotochemical Chl fluorescence quenching; qE, rapidly reversible component of NPQ; Nx, Neoxanthin; RRS, resonance Raman spectroscopy; Vx, violaxanthin.

* Corresponding author.
[1] These authors contributed equally to this work.
[2] These authors contributed equally to this work.

http://dx.doi.org/10.1016/j.bbabio.2016.06.001
0005-2728/

activity, as well as testing the different models for these mechanisms. In the case of LHCII, this task is particularly difficult, partially because of the degeneracy of the nuclear genes encoding its subunits. An alternative approach, pioneered by the work of Paulsen et al. [9], consists of expressing pea LHCII polypeptides in *Escherichia coli*, and reconstituting the protein by mixing the resulting apoproteins, solubilized in detergent solution, with the proper proportion of photosynthetic pigments. This approach is obviously complex, given the large number of cofactors that must find their proper place in the rapidly refolding protein, but it has been quite successful and found a large number of applications. Perhaps the most spectacular examples were the mechanistic analysis of LHC refolding *in vitro* [10] and the determination of the Nx binding site well in advance of the crystal structures [11] .

However, most of these studies concerned only monomeric LHCs — either the minor antenna proteins such as CP29, or reconstituted LHCII monomers. In its native form, LHCII is a trimer, and obtaining trimerised LHCII in its native conformation is a particularly daunting task [12]. This is significant, as while the overall shape of the monomer corresponds to that in the trimer, its spectroscopic properties show subtle differences from the native protein [13]. Recently, we reported reconstitution of LHCII trimers from WT and mutated apoproteins, where S123 was chosen as the site for point mutations due to its strategic position at the junction between helix C and the lumenal loop of LHCII [14,15]. Mutations at this locus were seen to induce small perturbations in the binding of Nx and some Chls *b* to the protein [15]. For instance, trimers reconstituted from polypeptides bearing the S123G mutation exhibited a reduction in neoxanthin and Chl *b* content of 20% & 7% respectively (the latter accounting for less than half a Chl *b* molecule per monomer), compared to WT reconstituted trimers with a near-to-native pigment stoichiometry [15]. In order to interpret the effect of single amino acid changes on LHCII function in reconstituted proteins, the quality of the reconstituted complexes as well as the structural impact of the mutation should be checked by as wide a range of techniques as possible. Among these techniques, a method of choice is resonance Raman spectroscopy (RRS), which has already been extensively applied to LHCII studies [16,17]. RRS provides selective vibrational information on the different types of pigments bound to the protein (Chls *a* & *b* and carotenoid molecules), according to the excitation wavelength used to produce the resonance effect [18]. As a vibrational method, it yields precise information on the molecular conformation, configuration and interactions of the excited pigment. Thus at wavelengths exciting Chl molecules, it can provide an exquisitely sensitive description of the interactions between the conjugated carbonyl groups of these pigments and their neighboring amino acids [19]. On the other hand, by progressively scanning the carotenoid absorption band with the Raman excitation, it was shown that this method may selectively provide structural information on the LHCII-bound Nx and on the red-absorbing lutein in these complexes [20]. This method can thus be used to evaluate the structure of reconstituted LHCII trimers, obtained from both WT and point-mutated apoproteins — indeed such measurements have already been used to investigate reconstituted CP29 [21,22]. Here we report a resonance Raman investigation of reconstituted WT and point-mutated LHCII trimers (mutations S123P & S123G). The precise location of this point mutation, in a loop connecting helices A and B to helix C, is shown in Fig. 1.

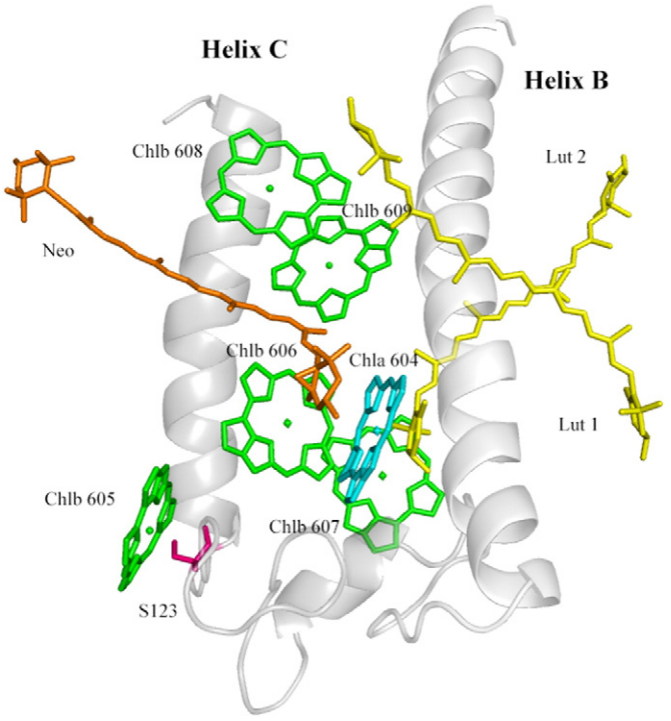


**Fig. 1.** Plausible structural model of reconstituted LHCII. Here we see five Chls b (green) and Chl b (cyan) are located near the Nx niche, which is effected by mutation of S123. The protein structure: part of α-helices B/C and the lumenal loop are gray. The related Chls (only shown with their porphyrin) and Cars, according to the nomenclature of Liu et al. [6]. The mutation site (Ser123) is presented in magenta.

## 2. Experimental procedures

### 2.1. Reconstitution of LHCII trimers

Expression, site-directed mutagenesis and reconstitution of the pea Lhcb1 apoprotein have been extensively described in Liu et al. [15]. Briefly, the apoprotein of different Lhcb1 species were overexpressed and isolated using the method described by Paulsen et al. [9]. LHCII was reconstituted according to [15] using a total thylakoid pigment extract. Absorption spectra of these reconstituted LHCIIs were similar to that reported in [14], as displayed in Fig. 2. The relative stoichiometry of the different pigments in these complexes was similar to previously reported data (not shown). Prior to resonance Raman measurements [15], reconstituted LHCII trimers were concentrated using 100 kDa centricon devices (Millipore) down to an OD of about 5 at 675 nm. For comparison, native LHCII were purified from spinach according to [23].

### 2.2. Pigment analysis

The bands corresponding to the trimeric LHCII were collected and the pigment extracted with 2-butylalcohol (Martinson 1995). The 2-

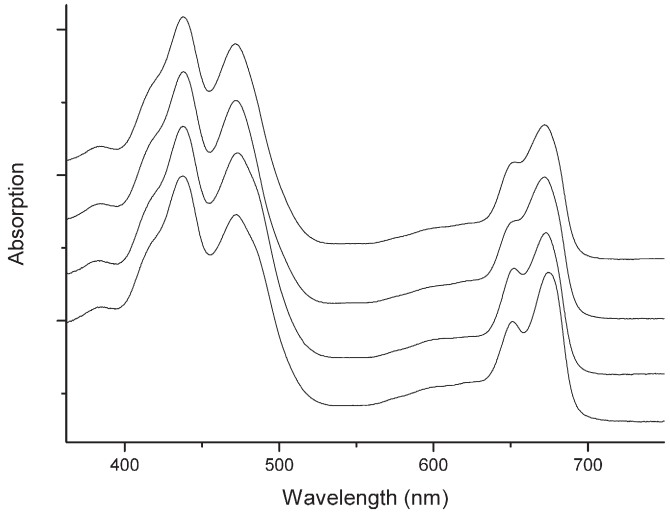


**Fig. 2.** Room temperature absorption spectra of (from bottom to top) purified native LHCII, LHCII reconstituted from WT lhcb1 apoprotein, S123P Lhcb1 apoprotein, and S123G Lhcb1 apoprotein.

butylalcohol extract was applied to an RP-C18 HPLC column (Agilent, America) and was eluted using methanol: acetonitrile 75: 25 for the first 9 min followed by a 3 min linear gradient to 100% of methanol:ethyl acetate 70:30.

### 2.3. Spectroscopy

Absorption spectra were collected using a Varian Cary E5 Double-beam scanning spectrophotometer. Resonance Raman spectra were recorded with 90° signal collection using a two-stage monochromator (U1000, Jobin Yvon, Longjumeau, France) equipped with a front-illuminated, deep-depleted CCD detector (Jobin Yvon, Longjumeau, France). Excitation wavelengths were provided by a 24 W Sabre Argon laser (514.5 & 488.0 nm; Coherent, Palo Alto, California), an Innova 90 Krypton laser (413.1 nm; Coherent, Palo Alto, California) and a Liconix helium–cadmium laser (441.6 nm); typically, less than 20 mW reached the sample. Measurements were performed at low temperature (77 K) using a nitrogen-flow cryostat (Air Liquide, Sassenage, France). Sample integrity was verified by following RR spectral evolution during the experiment, as well as measuring the fluorescence properties at the same place producing the Raman signal, using the Raman spectrometer as a fluorimeter.

## 3. Results

### 3.1. Pigment stoichiometries

Table 1 shows the pigment stoichiometries of the different LHCII used in this work. The stoichiometry of each pigment was calculated based on the assumption that each monomer binds 2 Luteins. Native LHCII bound *ca.* 1.00 Nx and the Chl *a*/*b* ratio is 1.22 as previously reported [15]. The pigment composition of the LHCII reconstituted from WT apoprotein is identical to the native, but does not bind violaxanthin, which was not provided during the reconstitution procedure. The LHCII reconstituted from the S123G and S123P mutated apoproteins bind a little less neoxanthin (10 and 30% less, respectively). The content of Chl *b* in LHCII reconstituted from the S123G apoprotein is similar to that of the purified LHCII, while the S123P mutation induces a slight loss of Chl *b* content (a bit less than one Chl *b* per trimer).

### 3.2. Lutein 2 in reconstituted LHCII

As stated above, resonance Raman provides detailed information on the molecular configuration of carotenoid molecules. Carotenoid resonance Raman spectra display four main groups of bands, denoted $\nu_1$ to $\nu_4$, which can be satisfactorily modelled in DFT calculations [24,25]. The $\nu_1$ band, of highest frequency, above 1500 $cm^{-1}$, arises from stretching vibrations of C═C double bonds [26]. Its position depends on the length of the π-electron conjugated chain and on the molecular configuration of the carotenoid [27–31]. The $\nu_2$ band around 1160 $cm^{-1}$ contains contributions from stretching vibrations of C—C single bonds coupled with C—H in-plane bending modes, and this region is a fingerprint for the assignment of carotenoid isomerization states [27,32]. The $\nu_3$ band (~1000 $cm^{-1}$) arises from in-plane rocking vibrations of the methyl groups attached to the conjugated chain, coupled with in-plane bending modes of the adjacent C—H's [26]. It was recently reported to be a fingerprint of the conjugated end-cycle configuration [25], a hypothesis confirmed by theoretical modelling [24]. Finally, the $\nu_4$ band around 960 $cm^{-1}$ arises from C—H out-of-plane wagging motions coupled with C═C torsional modes (out-of-plane twists of the carbon backbone) [26]. When the carotenoid conjugated system is planar, these out-of-plane modes will not be coupled with the electronic transition, and so these bands will not be resonance-enhanced. However, distortions around C—C single bonds will increase the coupling of these modes with the electronic transition, resulting in an increase in their intensity. Hence they can be used as an indicator of such distortions (twisting) of the carotenoid backbone — see *e.g.* [33].

In LHCII, trimerisation induces a redshift of the absorption position of one of the luteins, called lutein 2, bringing the lower energy component of the absorption transition of this molecule to 507 nm [20]. Excitation of these complexes at 514.5 nm results in near-to-selective excitation of this molecule [20]. Fig. 3 displays the resonance Raman spectra of native and reconstituted LHCII (for both WT and mutants). It is clear that these spectra are nearly identical. For LHCII purified from thylakoid membranes, the transition from trimer to monomer induces a 4 $cm^{-1}$ downshift of the $\nu_1$ band, from 1522 to 1526 $cm^{-1}$. This was recently interpreted as resulting from steric hindrances induced by the protein binding site upon trimerisation, forcing the partially-conjugated lutein end-cycle (the β-ring) into the conjugated plane, thus increasing the extent of its conjugation and shifting the absorption transition to the red [25]. These changes are accompanied by the appearance of two clear components in the $\nu_4$ band, at 955 and 965 $cm^{-1}$ [20]. LHCII monomers display only a broad, unstructured band in this region, and so this $\nu_4$ structure is typical for native LHCII trimers. It results from slight distortions of lutein 2 induced by the reorganization of its protein binding site upon trimerisation. The fact that these features are observed in the reconstituted LHCII trimers indicates that, in the complexes reconstituted from WT and mutant Lhcb1 apoprotein, trimerisation induces exactly the same constraints on the lutein 2 binding site as for native trimers (including the absorption redshift). This is a clear indicator of the quality of trimerisation achieved.

### 3.3. Neoxanthin in reconstituted LHCII

Because of its structure, the resonance Raman spectra of 9-*cis* Nx are slightly different from those of *all-trans* lutein. The shorter conjugation

**Table 1**
Pigment composition of LHC II complexes[a].

| Type of LHCIIb | Nx | Vx | Lutein | Chl *a* | Chl *b* | Chl *a*/*b* |
|---|---|---|---|---|---|---|
| Native | 1.05 ± 0.10 | 0.25 ± 0.02 | 2 | 7.51 ± 0.26 | 6.14 ± 0.17 | 1.22 |
| WT | 1.05 ± 0.02 | / | 2 | 7.11 ± 0.26 | 6.24 ± 0.20 | 1.14 |
| S123G | 0.94 ± 0.01 | / | 2 | 7.13 ± 0.35 | 5.93 ± 0.41 | 1.20 |
| S123P | 0.77 ± 0.03 | / | 2 | 7.32 ± 0.18 | 5.64 ± 0.25 | 1.30 |

[a] The stoichiometry of each pigment was calculated based on the assumption that each monomer binds 2 Lutein. Nx, Neoxanthin; Vx, Violaxanthin; /, trace.

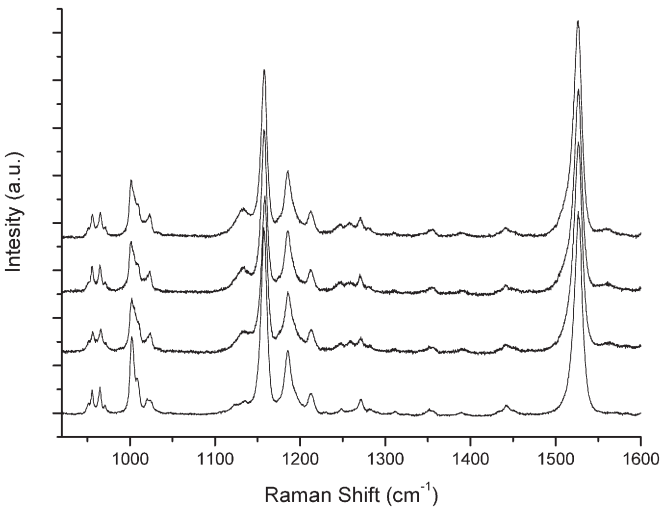


**Fig. 3.** Resonance Raman spectra (514.5 nm excitation, leading to lutein 2 contributions) of (from bottom to top) purified LHCII from spinach, LHCII reconstituted from WT Lhcb1 apoprotein from pea, LHCII reconstituted from S123P Lhcb1 apoprotein, and LHCII reconstituted with S123G Lhcb1 apoprotein. Spectral range displayed: 920–1600 $cm^{-1}$.

length for neoxanthin is accompanied by a small upshift in its $\nu_1$ band, while the presence of the 9-*cis* configuration results in the appearance of additional bands in the $\nu_2$ region (see below). Using these differences, it was proposed that the LHCII-bound Nx dominates the Raman spectra for excitations at 488 nm [20]. This proposal was fully confirmed by the study of LHCII from the *npq2* mutant of *Arabidopsis thaliana*, which is unable to synthesize Nx. In the 488 nm-excited resonance Raman spectra of *npq2* LHCII, the bands attributed to Nx were absent [34]. In the spectra of all three reconstituted LHCII proteins, displayed in Fig. 4, the additional bands in the $\nu_2$ region (indicated by arrows) clearly reveal the contribution of the 9-*cis* carotenoid. It was shown that the $\nu_4$ band of Nx, as excited at 488 nm, is particularly sensitive to the LHCII conformation, and gains intensity upon protein aggregation and/or detergent removal *in vitro*, and upon build-up of qE *in vivo* [4,18]. Fig. 5 displays this spectral region for the purified and reconstituted LHCIIs. While the spectral components in $\nu_4$ are identical for native LHCII and for the reconstituted WT and S123G, there is a clear change in this region for mutant S123P. In wild-type LHCII, three components appear at 954, 964 and 974 $cm^{-1}$, with relative intensities of 0.5, 1.0 and 0.3. In S123P, the component at 954 $cm^{-1}$ is broader and more intense, possibly containing an additional band at lower frequencies, while the highest-frequency component is down-shifted to 971 $cm^{-1}$ and slightly more intense. As this region corresponds to modes sensitive to Nx distortions, it may be concluded that the introduction of a proline at position 123 has an effect on the Nx conformation, due to a limited reorganization of the Nx binding pocket.

### 3.4. Chlorophyll b molecules

Resonance Raman spectra of Chl molecules contain bands which arise from those vibrational modes coupled with the electronic transition used to produce the resonance (usually the highest-energy Soret band, to avoid interference with the intrinsic fluorescence of Chl [35]). As extensively documented (see *e.g.* [36,37]) these modes generally arise from vibrations highly delocalized on the Chl macrocycle, some in the low-frequency range (around 300 $cm^{-1}$) which involve the central Mg atom, others in the high-frequency range (above 1630 $cm^{-1}$) arising almost purely from C═O stretching modes [38]. The modes involving the Mg atom are sensitive to the coordination state of this atom. A series of modes in the mid-frequency range has also been determined to be sensitive to the Chl macrocycle conformation [39,40]. However, none of these modes (including those at low

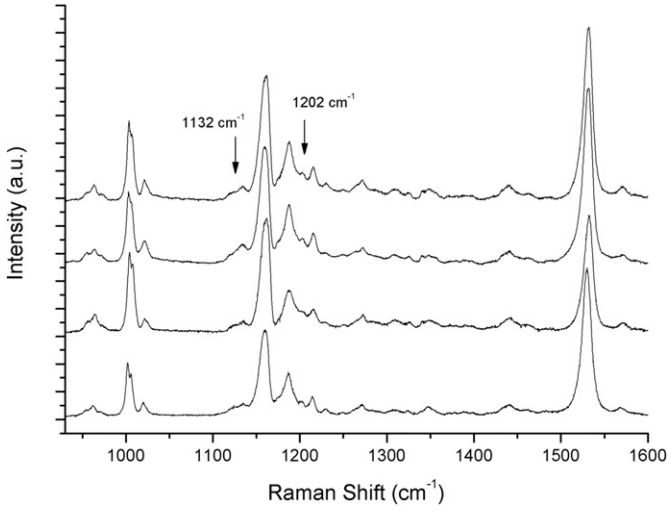


**Fig. 4.** Resonance Raman spectra (488.0 nm excitation, leading essentially to neoxanthin contributions) of (from bottom to top) purified LHCII from spinach, LHCII reconstituted from WT Lhcb1 apoprotein from pea, LHCII reconstituted from S123P Lhcb1 apoprotein, and LHCII reconstituted with S123G Lhcb1 apoprotein. Spectral range displayed: 930–1600 $cm^{-1}$.

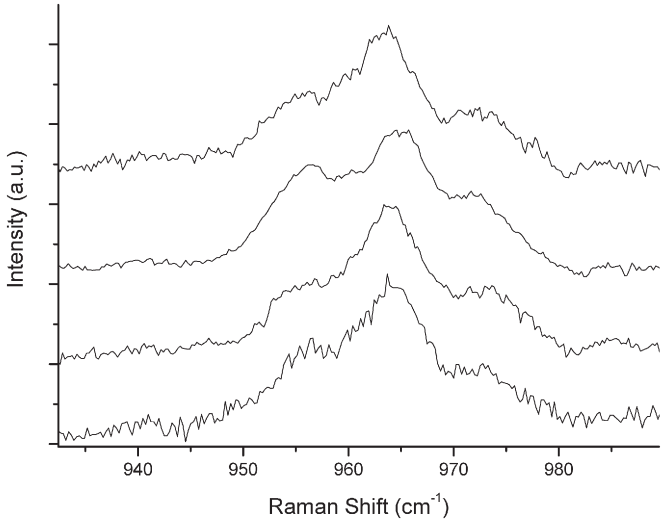


**Fig. 5.** $\nu_4$ region of Resonance Raman spectra (488.0 nm excitation) of (from bottom to top) purified LHCII from spinach, LHCII reconstituted from WT Lhcb1 apoprotein from pea, LHCII reconstituted from S123P Lhcb1 apoprotein, and LHCII reconstituted with S123G Lhcb1 apoprotein. Spectral range displayed: 930–990 $cm^{-1}$.

frequency) usually undergo frequency shifts large enough that they can be used for conclusive analysis of the Chls bound to proteins as complex as LHCII, containing as it does some 14 Chl molecules per monomer. In the high-frequency range, the stretching modes of conjugated C═O groups contribute (keto groups for Chl *a*; formyl and keto for Chl *b*) [41]. The keto stretching modes of Chl *a* and *b* contribute at *ca* 1700 $cm^{-1}$ when free-from-interactions, and this frequency may downshift to 1660 $cm^{-1}$ upon intermolecular interactions. Formyl carbonyl vibrates at 1660 $cm^{-1}$ when free from interactions, and may downshift to 1620 $cm^{-1}$ upon binding with surrounding partners. In both cases, the extent of the down-shift is determined by the strength of the interaction involved. An increase in polarity of the immediate environment of the carbonyl group can also result in a down-shift of its stretching frequency, but to a lesser extent (5–10 $cm^{-1}$).

The six LHCII-bound Chls *b*, with their formyl and keto carbonyls vibrating in two different frequency ranges, can thus provide detailed information on any structural changes experienced by this protein [3,18]. In order to evaluate the reconstituted WT and mutated LHCII, we compared the resonance Raman spectra of these complexes excited at 441.6 nm, where Chl *b* contributions dominate the spectra, in the carbonyl frequency region (Fig. 6). The spectra of all three reconstituted LHCII proteins are nearly identical, indicating that the interaction states of the Chls *b* are similar in these complexes. This may sound contradictory with the slight differences in Chl *b* stoichiometries observed in these complexes; however, this represents at most 6% of the total content of Chl *b* bound to the complexes, and such a small difference may actually not be clearly observed in the resonance Raman spectra. All these spectra differ slightly from those obtained for native LHCII. The formyl carbonyl stretching region of purified LHCII displays two main contributions at 1630 and 1640 $cm^{-1}$, reflecting two populations of formyl carbonyl groups, in interactions of differing strengths with neighboring partners. A small contribution at 1656 $cm^{-1}$ could correspond either to an additional free-from-interaction formyl group or to a strongly-bound keto carbonyl. At higher frequencies, a complex envelope of contributions is observed for keto carbonyl groups (in addition to 1656 $cm^{-1}$). The 1675 $cm^{-1}$ band arises from interacting keto C═O's, while at higher frequencies, between 1686 and 1705 $cm^{-1}$, contribute free-from-interaction keto carbonyls in different electrostatic environments [38]. These bands were tentatively attributed to Chl *a* keto stretching vibrations observed in pre-resonance [22], however, the fact that they are very similar when exciting in these resonance conditions, while a large difference is observed in the same spectral region

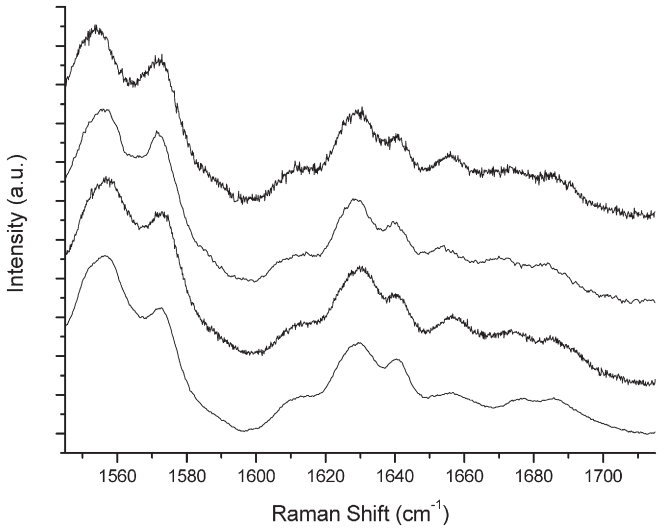


**Fig. 6.** Resonance Raman spectra (441.6 nm excitation, leading to Chl *b* contributions from bottom to top) purified LHCII from spinach, LHCII reconstituted from WT Lhcb1 apoprotein from pea, LHCII reconstituted from S123P Lhcb1 apoprotein, and LHCII reconstituted with S123G Lhcb1 apoprotein. Spectral range displayed: 1540–1715 $cm^{-1}$.

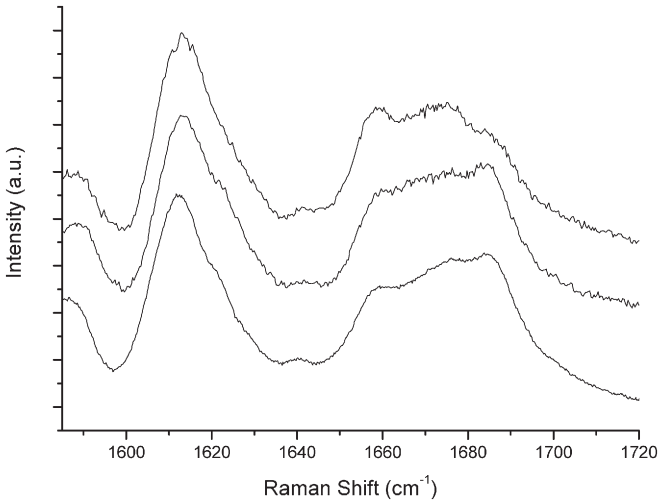


**Fig. 7.** Resonance Raman spectra (413.1 nm excitation, leading to Chl *a* contributions) of (from bottom to top) purified LHCII from spinach, LHCII reconstituted from WT Lhcb1 apoprotein from pea and LHCII reconstituted from S123P mutated Lhcb1 apoprotein. Spectral range displayed: 1480–1720 $cm^{-1}$.

when selectively exciting Chl *a* molecules (see below), indicates that they actually arise from Chl *b* keto carbonyl stretching modes. In the reconstituted complexes, the intensity of the 1640 $cm^{-1}$ band is decreased by 20%, while the 1656 $cm^{-1}$ contribution increases. This indicates that a number of Chl *b* molecules, whose formyl groups are involved in interactions in the native protein, are present in sites in the reconstituted complexes that are unable to provide their natural H-bonding partner. It must be noted that no decrease of the band at 1630 $cm^{-1}$ corresponding to the most strongly-bound formyl is observed, indicating optimized recruitment of and interaction with Chl *b* at these sites during the reconstitution procedure. Concerning the keto contributions, those corresponding to free-from-interaction carbonyls are very similar between the purified and reconstituted complexes. A small change in profile is observed around 1670 $cm^{-1}$, where the main contribution is down-shifted slightly for the reconstituted complexes, indicating the presence of keto carbonyl groups involved in slightly stronger H-bonds.

### 3.5. Chlorophyll a molecules

As stated above, the most sensitive Raman bands in Chl *a* spectra are those arising from the stretching modes of the conjugated C═O carbonyl groups of these molecules in the high frequency region of the spectra. These can be measured with high selectivity (*i.e.* to the exclusion of Chl *b* contributions) by using an excitation located on the high-energy side of the Chl *a* Soret band, around 400 nm. Fig. 7 displays the high frequency range of the resonance Raman spectra obtained with 413.1 nm excitation from purified and reconstituted LHCII complexes. Despite the high degree of congestion in the complex cluster of C═O stretching modes between 1648 and 1705 $cm^{-1}$, which indicates a number of non-equivalent keto carbonyl modes, the spectra obtained from the reconstituted WT protein look nearly identical to those of native LHCII. This indicates that, for LHCII trimers reconstituted from the WT protein, the Chl *a* molecules find their proper site in the protein and assume their native conformation and interactions in the binding pocket, at least for the very large majority. By contrast, the spectra for S123P trimers display a very clear and well-defined alteration. The component at 1656 $cm^{-1}$ appears to gain intensity, while the 1686 $cm^{-1}$ band becomes weaker. The extent of increase at 1656 $cm^{-1}$ appears to be similar to the area lost at 1686 $cm^{-1}$, and calculating the difference spectrum confirms that about 8% of the total area in the envelope of carbonyl stretching modes shifts from 1686 to 1656 $cm^{-1}$ (data not shown). Taking into account that 8 Chls *a* are bound per monomer, then approximately one Chl *a* molecule which is free from interactions in native LHCII finds an H-bonding partner in the S123P mutant. This finding is quite remarkable, as the room temperature absorption spectra of S123P trimer differ by less than 1% from the reconstituted WT [15].

## 4. Discussion

Resonance Raman analysis of reconstituted LHCII trimers yields a number of conclusions about the carotenoid conformation of these complexes. When the reconstitution is performed using either WT or S123G apoproteins, the conformation of the lutein 2 and Nx molecules is exactly the same as those in purified LHCII, indicating that the structure of these carotenoid binding pockets is identical in all three complexes. For Nx this is quite surprising, as the amount of Nx bound to the S123G mutant (Table 1) is somewhat lower than in the WT [15]. This indicates that, where Nx is bound to the S123G apoprotein, it does so in its native state. To put it another way, either a Nx molecule binds exactly as *in vivo*, or it does not bind at all — no non-native binding conformation is possible. As lutein 2 is deeply embedded in the protein, running from one side of protein to the other at the level of helices A and B, while Nx is in close contact with helix C, this indicates that the folding in reconstituted LHCII is identical to that of the native protein at the level of its entire *trans*-membrane domain. Since resonance Raman is extremely sensitive to slight distortions of the C═C conjugated chain, this actually indicates that the detailed structure of these reconstituted complexes is very similar, if not identical, to that of purified LHCII. In all three reconstituted proteins, the Chl *b* interactions are observed to be extremely similar to each other, but slightly different from those observed in purified LHCII. The main conclusion is that a small number of Chls *b* are located in sites unable to provide the natural partner of their formyl carbonyl. The exact number of misallocated Chls *b* is not easy to determine from the Raman spectra, as many factors may influence the intensity of the carbonyl stretching modes, such as their geometry or binding state or the precise position of the absorption transition involved in resonance. However, considering the overall intensity changes in the carbonyl stretching region, these changes should affect between 10 and 20% of the LHCII-bound Chls *b*, *i.e.* about half a chlorophyll molecule per LHCII monomer. The presence of "promiscuous" Chl-binding sites, that may accommodate Chl *a* or Chl *b*, is well documented for reconstituted CP29 complexes [22]; these sites are occupied selectively by Chl *a* or Chl *b* in the crystal structure

[42]. Since Chl *a* has no formyl carbonyl, a limited number of Chls *b* located in Chl *a* sites (where no partner for the formation of formyl carbonyl is present), would fully explain our resonance Raman spectra. As the intensity of the 1630 $cm^{-1}$ is the same for all studied complexes, we may further conclude that the missing (or exchanged) Chls *b* are not those which have the stronger interaction with the surrounding protein. On the other hand, it is quite surprising that all the reconstituted complexes display similar resonance Raman spectra, despite the reported variation in Chl *b* content between trimers reconstituted from WT and those from S123G & S123P apoproteins [15]. However, the overall change was about 7% of the total bound Chl *b*, and if this change is scattered over a large number of Chl populations, this could be difficult to observe in the resonance Raman spectra. Finally, the data obtained show that the Chl *a* molecules are likely to find their proper binding sites in the LHCII reconstituted from the WT apoprotein, and that one specific Chl *a* has a carbonyl changing interaction state in the S123P mutant.

The close similarity between the structures of LHCII reconstituted from different apoproteins may help in addressing the influence of the pigment binding sites on the electronic properties of bound chromophores. In the spectra of S123P trimers, we observe two major structural differences relative to those reconstituted with WT or S123G apoproteins, affecting the Nx-binding site on one hand, and one Chl *a*-binding site on the other. Introduction of a proline at position 123 has a limited but significant effect on the Nx conformation, observed as a change in the intensity of C—H out-of-plane wagging motions coupled with C═C torsional modes for excitation at 488 nm. Although these spectra are dominated by Nx contributions, the selectivity relative to lutein is only partial. Thus, the effect of this distortion on the other Raman bands is difficult to estimate. It is worth comparing the absorption spectra of LHCII reconstituted with S123G and S123P apoproteins. Absorption difference spectra obtained between these two samples show an S-shaped signal centered at 482 nm, the maximum position expected for Nx (Fig. 8). It is thus likely that the additional distortion observed in the S123 P mutant is accompanied by a slight blueshift of the Nx absorption. On the other hand, the change in stretching frequency of the keto carbonyl group of a Chl *a*, from 1686 to 1656 $cm^{-1}$, which corresponds to the formation of a strong H-bond between this group and its environment, does not seem to have a measurable effect on LHCII absorption. Thus, we may safely conclude that the interaction state of Chl keto carbonyls has little if any influence on their absorption properties. A similar conclusion was proposed in the particular case of strongly-interacting bacteriochlorophyll molecules, using LH2 mutants [43]. Thus the use of reconstituted mutants has allowed us, for the first time, to obtain a precise conclusion about the structural parameters which may (or may not) play a role in tuning Chl molecules in LHCII and more generally in photosynthetic proteins from oxygen-evolving organisms.

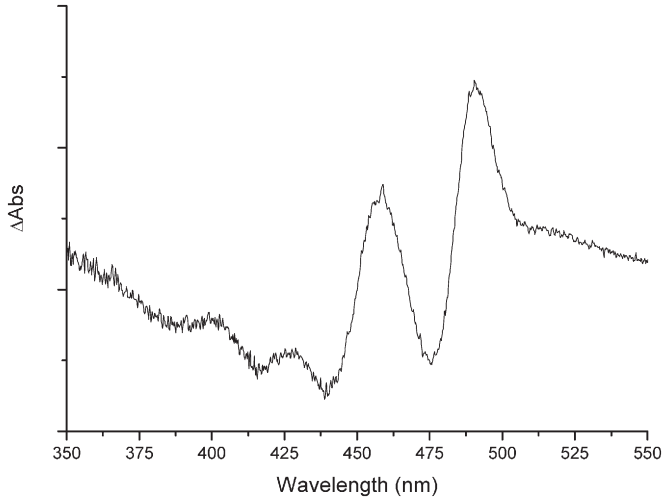


**Fig. 8.** Absorption difference spectra obtained for LHCII reconstituted with S123G apoproteins minus LHCII reconstituted with S123P.

## Transparency document

The Transparency document associated with this article can be found, in online version.

## Acknowledgements

This work was supported by the European Research Council (http://erc.europa.eu/) through the Advanced Grant PHOTPROT (contract number 267333); the French Infrastructure for Integrated Structural Biology www.structuralbiology.eu/networks/frisbi (grant number ANR-10-INSB-05-01); the CEA interdisciplinary program Technology for Health (MEDIASPEC project); the National Basic Research Program of China (Grant No. 2011CBA00904), and the Key Research Program of the Chinese Academy of Sciences Grant (KSZD-EW-Z-018).

## References

[1] H. Kirchhoff, Architectural switches in plant thylakoid membranes, Photosynth. Res. 116 (2013) 481–487.
[2] P. Horton, A.V. Ruban, D. Rees, A.A. Pascal, G. Noctor, A.J. Young, Control of the light-harvesting function of chloroplast membranes by aggregation of the LHCII chlorophyll — protein complex, FEBS Lett. 292 (1991) 1–4.
[3] A.A. Pascal, Z. Liu, K. Broess, B. van Oort, H. van Amerongen, C. Wang, P. Horton, B. Robert, W. Chang, A. Ruban, Molecular basis of photoprotection and control of photosynthetic light-harvesting, Nature 436 (2005) 134–137.
[4] A.V. Ruban, R. Berera, C. Ilioaia, I.H.M. van Stokkum, J.T.M. Kennis, A.A. Pascal, H. van Amerongen, B. Robert, P. Horton, R. van Grondelle, Identification of a mechanism of photoprotective energy dissipation in higher plants, Nature 450 (2007) 575–578.
[5] B.R. Green, D. Shen, R. Aebersold, E. Pichersky, Identification of the polypeptides of the major light-harvesting complex of photosystem II (LHCII) with their genes in tomato, FEBS Lett. 305 (1992) 18–22.
[6] Z. Liu, H. Yan, K. Wang, T. Kuang, J. Zhang, L. Gui, X. An, W. Chang, Crystal structure of spinach major light-harvesting complex at 2.72 A resolution, Nature 428 (2004) 287–292.
[7] J. Standfuss, A.C. Terwisscha van Scheltinga, M. Lamborghini, W. Kühlbrandt, Mechanisms of photoprotection and nonphotochemical quenching in pea light-harvesting complex at 2.5 Å resolution, EMBO J. 24 (2005) 919–928.
[8] V.I. Novoderezhkin, R. van Grondelle, Physical origins and models of energy transfer in photosynthetic light-harvesting, Phys. Chem. Chem. Phys. 12 (2010) 7352–7365.
[9] H. Paulsen, U. Rümler, W. Rüdiger, Reconstitution of pigment-containing complexes from light-harvesting chlorophyll *a*/b-binding protein overexpressed in *Escherichia coli*, Planta 181 (1990) 204–211.
[10] E. Giuffra, D. Cugini, R. Croce, R. Bassi, Reconstitution and pigment-binding properties of recombinant CP29, Eur. J. Biochem. 238 (1996) 112–120.
[11] R. Croce, R. Remelli, C. Varotto, J. Breton, R. Bassi, The neoxanthin binding site of the major light harvesting complex (LHCII) from higher plants, FEBS Lett. 456 (1999) 1–6.
[12] S. Hobe, S. Prytulla, W. Kühlbrandt, H. Paulsen, Trimerization and crystallization of reconstituted light-harvesting chlorophyll *a*/b complex, EMBO J. 13 (1994) 3423–3429.
[13] E.J. Peterman, F.M. Dukker, R. van Grondelle, H. van Amerongen, Chlorophyll a and carotenoid triplet states in light-harvesting complex II of higher plants, Biophys. J. 69 (1995) 2670–2678.
[14] L. Zhang, T.B. Melø, H. Li, K.R. Naqvi, C. Yang, The inter-monomer interface of the major light-harvesting chlorophyll *a*/b complexes of photosystem II (LHCII) influences the chlorophyll triplet distribution, J. Plant Physiol. 171 (2014) 42–48.
[15] C. Liu, Y. Zhang, D. Cao, Y. He, T. Kuang, C. Yang, Structural and functional analysis of the antiparallel strands in the lumenal loop of the major light-harvesting chlorophyll a/b complex of photosystem II (LHCIIb) by site-directed mutagenesis, J. Biol. Chem. 283 (2008) 487–495.
[16] B. Robert, Resonance Raman spectroscopy, Photosynth. Res. 101 (2009) 147–155.
[17] A. Gall, A.A. Pascal, B. Robert, Vibrational techniques applied to photosynthesis: resonance Raman and fluorescence line-narrowing, Biochim. Biophys. Acta Bioenerg. (2014).
[18] A.V. Ruban, P. Horton, B. Robert, Resonance Raman spectroscopy of the photosystem II light-harvesting complex of green plants: a comparison of trimeric and aggregated states, Biochemistry 34 (1995) 2333–2337.
[19] B. Robert, Resonance Raman studies of bacterial reaction centers, Biochim. Biophys. Acta Bioenerg. 1017 (1990) 99–111.
[20] A.V. Ruban, A.A. Pascal, B. Robert, Xanthophylls of the major photosynthetic light-harvesting complex of plants: identification, conformation and dynamics, FEBS Lett. 477 (2000) 181–185.

[21] A. Pascal, M. Gastaldelli, S. Ceoldo, R. Bassi, B. Robert, Pigment conformation and pigment–protein interactions in the reconstituted Lhcb4 antenna protein, FEBS Lett. 492 (2001) 54–57.
[22] R. Bassi, R. Croce, D. Cugini, D. Sandonà, Mutational analysis of a higher plant antenna protein provides identification of chromophores bound into multiple sites, Proc. Natl. Acad. Sci. 96 (1999) 10056–10061.
[23] A.V. Ruban, A.J. Young, A.A. Pascal, P. Horton, The effects of illumination on the xanthophyll composition of the photosystem II light-harvesting complexes of spinach thylakoid membranes, Plant Physiol. 104 (1994) 227–234.
[24] M. Macernis, J. Sulskus, S. Malickaja, B. Robert, L. Valkunas, Resonance Raman spectra and electronic transitions in carotenoids: a density functional theory study, J. Phys. Chem. A 118 (2014) 1817–1825.
[25] M.M. Mendes-Pinto, D. Galzerano, A. Telfer, A.A. Pascal, B. Robert, C. Ilioaia, Mechanisms underlying carotenoid absorption in oxygenic photosynthetic proteins, J. Biol. Chem. 288 (2013) 18758–18765.
[26] S. Saito, M. Tasumi, Normal-coordinate analysis of retinal isomers and assignments of Raman and infrared bands, J. Raman Spectrosc. 14 (1983) 236–245.
[27] Y. Koyama, T. Takii, K. Saiki, K. Tsukida, Configuration of the carotenoid in the reaction centers of photosynthetic bacteria. 2. Comparison of the resonance Raman lines of the reaction centers with those of the 14 different *cis*-trans isomers of β-carotene, Photochem. Photobiol. 5 (1983) 139–150.
[28] Y. Koyama, R. Fujii, *Cis*-trans carotenoids in photosynthesis: configurations, excited-state properties and physiological functions, in: H.A. Frank, A.J. Young, G. Britton, R.J. Cogdell (Eds.), The Photochemistry of Carotenoids, Springer Netherlands 1999, pp. 161–188.
[29] L. Rimai, M.E. Heyde, D. Gill, Vibrational spectra of some carotenoids and related linear polyenes. Raman spectroscopic study, J. Am. Chem. Soc. 95 (1973) 4493–4501.
[30] Y. Koyama, M. Kito, T. Takii, K. Saiki, K. Tsukida, J. Yamashita, Configuration of the carotenoid in the reaction centers of photosynthetic bacteria. Comparison of the resonance Raman spectrum of the reaction center of *Rhodopseudomonas sphaeroides* G1C with those of *cis*-trans isomers of β-carotene, Biochim. Biophys. Acta Bioenerg. 680 (1982) 109–118.
[31] Y. Koyama, I. Takatsuka, M. Nakata, M. Tasumi, Raman and infrared spectra of the all-trans, 7-cis, 9-cis, 13-cis and 15-cis isomers of β-carotene: key bands distinguishing stretched or terminal-bent configurations form central-bent configurations, J. Raman Spectrosc. 19 (1988) 37–49.
[32] V.R. Salares, N.M. Young, P.R. Carey, H.J. Bernstein, Excited state (excitation) interactions in polyene aggregates. Resonance Raman and absorption spectroscopic evidence, J. Raman Spectrosc. 6 (1977) 282–288.
[33] M. Lutz, W. Szponarski, G. Berger, B. Robert, J.-M. Neumann, The stereoisomerization of bacterial, reaction-center-bound carotenoids revisited: an electronic absorption, resonance Raman and NMR study, Biochem. Biophys. Acta 894 (1987) 423–433.
[34] C. Ilioaia, M.P. Johnson, P.-N. Liao, A.A. Pascal, R. van Grondelle, P.J. Walla, A.V. Ruban, B. Robert, Photoprotection in plants involves a change in lutein 1 binding domain in the major light-harvesting complex of photosystem II, J. Biol. Chem. 286 (2011) 27247–27254.
[35] M. Lutz, Antenna chlorophyll in photosynthetic membranes. A study by resonance Raman spectroscopy, Biochim. Biophys. Acta Bioenerg. 460 (1977) 408–430.
[36] A. Telfer, A.A. Pascal, L. Bordes, J. Barber, B. Robert, Fluorescence line narrowing studies on isolated chlorophyll molecules, J. Phys. Chem. B 114 (2010) 2255–2260.
[37] M. Ceccarelli, M. Lutz, M. Marchi, A density functional normal mode calculation of a bacteriochlorophyll a derivative, J. Am. Chem. Soc. 122 (2000) 3532–3533.
[38] K. Lapouge, A. Näveke, J.N. Sturgis, G. Hartwich, D. Renaud, I. Simonin, M. Lutz, H. Scheer, B. Robert, Non-bonding molecular factors influencing the stretching wavenumbers of the conjugated carbonyl groups of bacteriochlorophyll a, J. Raman Spectrosc. 29 (1998) 977–981.
[39] M. Fujiwara, M. Tasumi, Resonance Raman and infrared studies on axial coordination to chlorophylls a and b in vitro, J. Phys. Chem. 90 (1986) 250–255.
[40] K. Lapouge, A. Näveke, A. Gall, A. Ivancich, J. Seguin, H. Scheer, J.N. Sturgis, T.A. Mattioli, B. Robert, Conformation of bacteriochlorophyll molecules in photosynthetic proteins from purple bacteria, Biochemistry 38 (1999) 11115–11121.
[41] U. Feiler, T.A. Mattioli, I. Katheder, H. Scheer, M. Lutz, B. Robert, Effects of vinyl substitutions on resonance Raman spectra of (bacterio)chlorophylls, J. Raman Spectrosc. 25 (1994) 365–370.
[42] X. Pan, M. Li, T. Wan, L. Wang, C. Jia, Z. Hou, X. Zhao, J. Zhang, W. Chang, Structural insights into energy regulation of light-harvesting complex CP29 from spinach, Nat. Struct. Mol. Biol. 18 (2011) 309–315.
[43] L.G. Kwa, A. García-Martín, A.P. Végh, B. Strohmann, B. Robert, P. Braun, Hydrogen bonding in a model bacteriochlorophyll-binding site drives assembly of light harvesting complex, J. Biol. Chem. 279 (2004) 15067–15075.